Spectroscopy Sleuth - An investigation of Telescopic Spectrometers through the Balmer Series

Diego Aguirre
Cornell University, College of Engineering
(7 May, 2024)

When a hydrogen lamp is powered on and aimed at a 600mm diffraction grating, emitted photons strike the grating and disperse outwards forming an emission spectrum. A spectrometer can then be used to measure the angular position of these spectral lines, from which their wavelengths can be computed. A value for the Rydberg Constant can then be extracted from each wavelength. Thirty of these values were computed yielding a mean of 10,951,400 1/m ∓ 88,453.6 (1/m)..

I. Intro

As you read this very text, countless photons are colliding with your retina, enabling your brain to render your surroundings. The behavior of these photons and the discovery of their discrete energy levels have revolutionized our understanding of Atomic Theory and the development of Quantum Mechanics. Originally discovered by Johannes Rydberg in 1890, the Rydberg Constant directly determines the wavelengths of the spectral lines of Hydrogen and similar ions. As such, its value governs a plethora of phenomena ranging from the size of atomic radii to optical instrument performance.

By aiming a hydrogen lamp at a 600mm diffraction grating, incident photons are dispersed outwards - forming the hydrogen spectra. A fine-tuned spectrometer with a Gaussian eye-piece can then be used to record their angular positions by centering each spectral line in its cross hair, and recording the corresponding vernier scale values. A value for the Rydberg constant can then be derived.

II. Theory

When hydrogen atoms are exposed to an electric current, their electrons enter an excited state and climb to a higher energy level. As these electrons drop back down to lower energy levels, their excess energy is emitted as a photon. When photons pass through the slits of a diffraction grating the majority are reflected and diffracted causing each slit to function as an individual point source. Due to the proximity of these slits, a large amount of interference occurs. At certain angles, constructive interference occurs and visible peaks form, and at others - destructive interference causes invisible troughs.

Following Thomas Young, we know that constructive interference only occurs if the following condition is satisfied:

$$\Delta s = m\lambda \qquad (1)$$

where Δs is the path difference between two waves, m is an integer, and λ is the wavelength. As such, the angular position of each peak is dependent on the wavelength of the incident photons. Applying the grating equation:

$$\lambda = dsin\theta \qquad (2)$$

where d is the grating spacing, and θ is the angle at which light is diffracted, we can relate the angular position of a peak to the wavelength of its photons. Each wavelength corresponds to a different energy level change.

Following the work of Rydberg, we observe that the specific relationship is governed by:

$$\frac{1}{\lambda} = R\left(\frac{1}{n_1^2} - \frac{1}{n_2^2}\right) \qquad (3)$$

where n_i are the energy states and R is the Rydberg Constant.

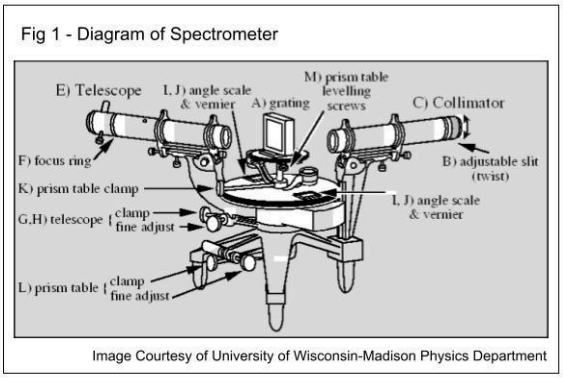

Fig 1. Overview of the telescopic spectrometer that was used throughout the experiment. A 600mm diffraction grating was used.

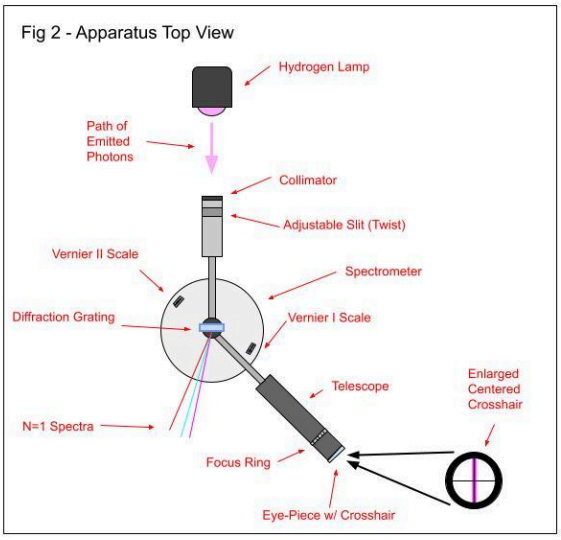

Fig 2. Overview of the layout. The collimator was aimed at the hydrogen lamp ensuring that emitted photons would strike the diffraction grating. The telescope arm would then be adjusted until the spectra was maximally centered.

Fig 3 - Table of Measured Angles and Computed Values

Color	Left Angle	Right Angle	Vernier	Theta (deg)	Theta (rad)	Lambda (m)	Rydberg (1/m)
violet	196.97	150.07	1	23.450	0.26625	6.6325e-07	10859000
violet	196.99	150.11	1	23.440	0.26642	6.6299e-07	10852000
violet	196.98	150.09	1	23.445	0.26608	6.6311e-07	10866000
violet	197.00	150.13	1	23.435	0.26590	6.6285e-07	10873000
violet	196.95	150.05	1	23.450	0.26616	6.6325e-07	10862000
violet	16.82	330.50	2	156.840	2.87580	6.5546e-07	10873000
violet	16.78	330.45	2	156.840	2.87630	6.5546e-07	10897000
violet	16.85	330.50	2	156.830	2.87600	6.5577e-07	10883000
violet	16.84	330.54	2	156.850	2.87610	6.5531e-07	10887000
violet	16.80	330.49	2	156.850	2.87630	6.5531e-07	10894000
red	190.41	156.74	1	16.835	0.40928	4.8270e-07	10856000
red	190.42	156.75	1	16.835	0.40911	4.8270e-07	10860000
red	190.40	156.72	1	16.840	0.40919	4.8283e-07	10858000
red	190.43	156.70	1	16.865	0.40902	4.8353e-07	10862000
red	190.46	156.77	1	16.845	0.40928	4.8297e-07	10856000
red	10.27	336.68	2	163.210	2.73740	4.8136e-07	10984000
red	10.31	336.70	2	163.200	2.73740	4.8168e-07	10982000
red	10.29	336.69	2	163.200	2.73720	4.8168e-07	10977000
red	10.31	336.72	2	163.210	2.73750	4.8136e-07	10988000
red	10.23	336.66	2	163.220	2.73750	4.8120e-07	10986000
cyan	188.78	158.27	1	15.255	0.29383	4.3853e-07	11049000
cyan	188.78	158.25	1	15.265	0.29383	4.3880e-07	11049000
cyan	188.79	158.30	1	15.245	0.29391	4.3825e-07	11046000
cyan	188.76	158.29	1	15.235	0.29435	4.3796e-07	11030000
cyan	188.76	158.26	1	15.250	0.29400	4.3838e-07	11043000
cyan	8.72	338.25	2	164.770	2.84860	4.3779e-07	11075000
cyan	8.69	338.29	2	164.800	2.84840	4.3699e-07	11068000
cyan	8.75	338.31	2	164.780	2.84840	4.3747e-07	11071000
cyan	8.70	338.27	2	164.790	2.84860	4.3731e-07	11075000
cyan	8.68	338.27	2	164.800	2.84870	4.3699e-07	11081000

Fig 3. Table containing the 30 measured Rydberg Constant values and their intermediates.

III. Apparatus

Our apparatus consists of two main components: a spectrometer as outlined in *Fig 1,* and a hydrogen lamp. Mounted to the spectrometer's base is a collimator aimed at the diffraction grating in the device's middle. The collimator constricts the incoming beams to ensure that the waves incident upon the diffraction grating are parallel . Mounted to the opposite side is a high precision rotatable arm with a telescope and gaussian eyepiece. The spectrometer has two vernier scales that measure the angle between the telescope's crosshair and the collimator. As outlined in *Fig 1,* there are various knobs and clamps that can be used to finetune and align the spectrometer. *Fig 2* overviews the general arrangement of the lamp and spectrometer. The collimator is aimed at the hydrogen lamp, and the telescope arm is then adjusted until the spectral line is centered in its crosshair.

IV. Experiment

The central goal of this experiment was to create a set of ~30 Rydberg constant values and compute their mean and standard deviation. This was accomplished by taking 5 rounds of 6 measurements across two data-collection sessions. Before delving into the specifics of each measurement round, it is important to note that the spectrometer was already finetuned and calibrated by a third party in advance to the start of the experiment. Prior to executing data collection, the only additional finetuning that occurred were adjusting the slit size and angle. In order to verify the degree of calibration, confirmatory

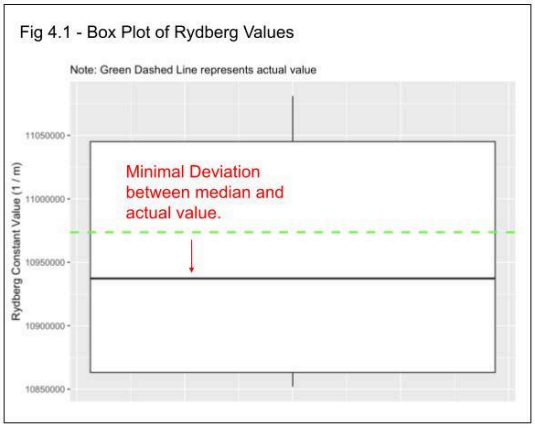

Fig 4.1. Boxplot of the 30 measured Rydberg Constant Values. We observe minimal deviation between the median measured value and the accepted value. The median and accepted value are roughly centered within the IQR.

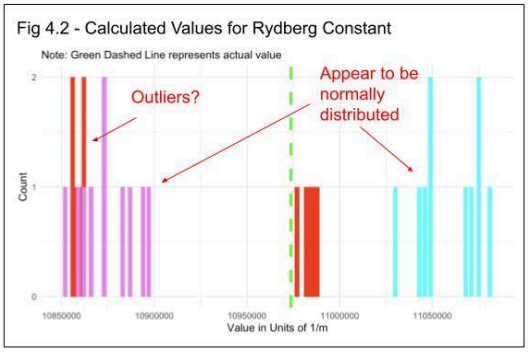

Fig 4.2. Distribution of the 30 measured values by Color. The values derived from the Cyan & Violet spectra appear to be normally distributed. Values derived from the red spectra have the highest variance, but also yield maximal precision.

calculations were run after each of the initial 3 rounds of data collection.

For each round, the following process was utilized. First, the hydrogen lamp was turned on and the remaining lights in the room were lowered. The telescope arm was aligned centrally with the diffraction grating, and then slowly panned to the right until the violet H_γ line was visible and centered in the crosshair. To minimize parallax the observer would sit at a low height and rest their chin on the table ensuring that their dominant eye was aligned with and nearly touching the telescope's eyepiece. The observer would then slowly slide their chin backwards in a straight line until the crosshair was in focus. This ensured that the observer's vantage point was consistently centered for each measurement. After H_γ was centered, the laboratory lights were turned back on, and a high resolution 48mp camera was used to photograph the vernier scales. The laboratory lights were then powered off, and the telescope arm was slowly panned to the right until the cyan H_β line was centered in the cross hair. The laboratory lights were then turned on, and the vernier scales were photographed again.

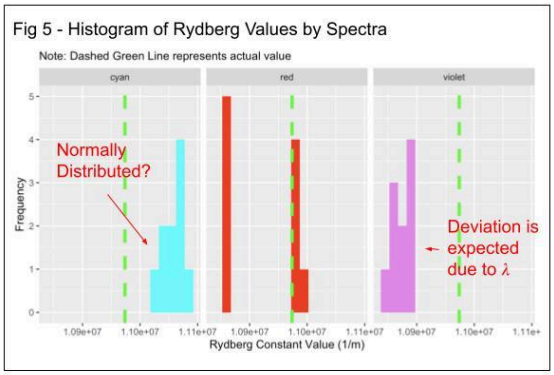

Fig 5. Histogram of the measured Rydberg Values by spectra. The facets make it easy to analyze each distribution. We observe "large" deviations from the accepted value in the sample derived from the violet spectra.

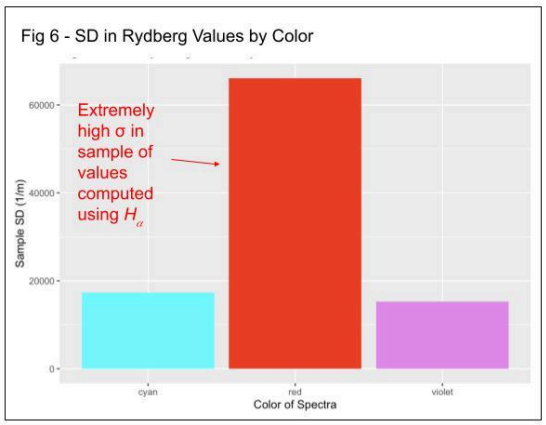

Fig 6. Bar chart of the standard deviations for each sample of measured Rydberg values. Due to its distinct clusters, the sample of values derived from the red spectra have the largest standard deviation.

Once more the lab lights were turned off and the telescope arm was slowly panned to the right until the red H_α line was centered. Its angular position was recorded by turning the lab lights back on, and then photographing the vernier scales. The telescope arm was then returned to its central position, and the same process was followed for the left H_γ , H_β , and H_α spectral lines. Every round yielded 6 photographs for the right spectra, and 6 photographs for the left spectra - from which 6 precise values for θ could be extracted.

The extraction process itself was lengthy. First the least count L_s of the spectrometer's scale was derived via:

$$L_s = L_m / L_v \qquad (4)$$

where L_m is the smallest division on the main scale , and L_v is the number of divisions on the vernier scale. Each angle value F_r was measured using the vernier scale equation:

$$F_r = MSR + (VSR \times L_s) \qquad (5)$$

where *MSR* is the main scale reading and *VSR* is the smallest vernier scale value that aligns with a main scale tick. In order to obtain *MSR* and *VSR* values, each image

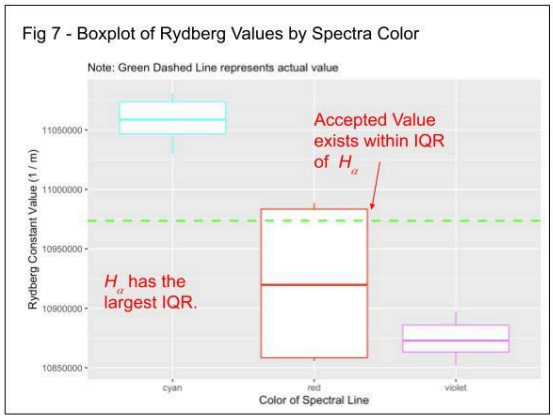

Fig 7. Boxplot of each sample of Rydberg Constant Values. The red spectra is the only spectra who's IQR included the accepted value. The deviation of the cyan spectra values is less than that of the violet spectra.

was opened in google drawings on a 27" monitor and scaled up. The *MSR* was measured as the outer scale value that aligned with the innerscale's zeroth mark. In order to increase the precision of this measurement, a 10 point ruler was overlaid onto the image such that it spanned the distance between the two outer scale marks that sandwiched the innerscale's zeroth mark. The *VSR* was the smallest inner scale value that aligned with any outer scale marks. The *VSR* was determined by first identifying a set of plausible overlaps, and then maximally zooming in on each to determine which one was actually aligned. Once the *VSR* value was denoted, the angular value F_r could be computed via *equation (5)*.

Since each measurement involved visually centering a spectral line, conducting Uncertainty Analysis proved to be rather troublesome. To remedy this, 5 rounds of data were collected resulting in a total of 30 measured values for the Rydberg Constant. The mean and standard deviation of this sample were computed, and by applying the Central Limit Theorem the sample mean was denoted as the final value, and the sample standard deviation was its uncertainty.

V. Results

The central result of this experiment was a set of 30 distinct values for the Rydberg Constant which were computed by measuring the angular positions of the Balmer Spectrum Lines 5 times. For each spectral color, the angle of the right and left spectral lines were recorded on both vernier scales. Their difference was taken and divided by 2, with the resultant value being denoted as θ. In order to calculate λ, each θ value was input into *equation (2)*. Since a 600mm diffraction grating was used, $d = 1.667$ micrometers. Each resultant λ value was then input into *equation (3)* along with the corresponding energy level states for the spectral line.This yielded 30 distinct

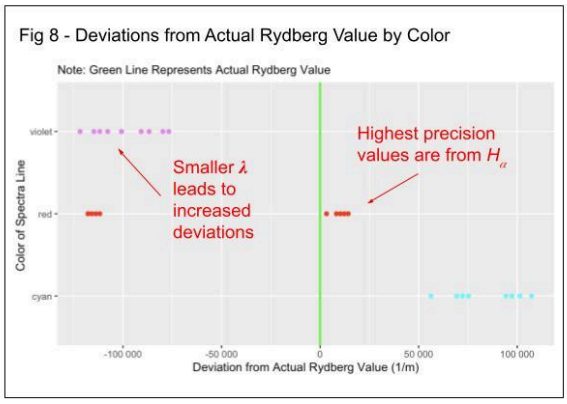

Fig 8. Plot of the deviations from the accepted value by spectral line. There is increased variance in the values derived from the red spectra. This is likely attributed to the calibration and precision of the spectrometer.

Fig 9 - Vernier Scale Analysis by Color

Color	Mean Theta Vern 1	Mean Theta Vern 2	% Difference
cyan	15.250	15.212	0.24949
red	16.844	16.792	0.30919
violet	23.444	23.158	1.22740

color	Mean R Vern 1	Mean R Vern 2	% Difference
cyan	11043400	11074000	0.2770886
red	10858400	10983400	1.1511825
violet	10862400	10886800	0.2246281

Fig 9. Table containing the mean values yielded by each Vernier Scale. Vernier Scale 2 consistently yielded larger θ values than Vernier Scale 1. Additionally, the discrepancy between small % difference in θ values for the red spectra and the large % difference in its final Rydberg values imply that the increased variance was likely attributed to systematic error and a lack of precision.

Rydberg Constant values, with a mean of 10,951,400 (1/m) and a standard deviation of 88,543.6 (1/m). Each of these values and their intermediates are contained in *Fig 3*.

Fig 4.1 shows a boxplot of these values, and *Fig 4.2* shows the distribution of these values by color. Interestingly, groupings by color occur. This phenomenon is logical, as the precision of our spectrometer varies by wavelength. Additionally, we note that a cluster of values from the red H_α line yielded higher precision than the values derived from the H_γ and H_β spectral lines. This too is logical, for the smaller wavelengths of the H_γ and H_β lines increase the amount of resolution that is required to yield precise measurements. However, it is also important to note that there is another cluster of values computed from the H_α line that have a far larger deviation from the accepted value.

Fig 5 captures this by plotting the frequencies of measured values by their corresponding spectral line. Measured values from the H_γ and H_β spectral lines have relatively uniform normal distributions, whereas the H_α line has more variance. *Fig 6* illustrates this increase in variance, as it plots the standard deviation of the computed Rydberg Constant values by Spectral Color. We observe that the standard deviation of the values derived from the H_α is over 3 times larger than that of the H_γ and H_β lines.

Fig 7 displays the IQR and mean of each sample of Rydberg Constant Values by spectral line. H_α is the only line who's IQR included the actual Rydberg Constant Value. *Fig 8* plots the deviations from the actual Rydberg Constant value for each spectral line. Mirroring *Fig 4.2* & *Fig 5,* the cluster of values that achieved the highest precision are from the H_α line. According to the Rayleigh Criterion, resolution improves with longer wavelengths. As such, red light tends to produce sharper and more distinct spectral features. This also explains why the cyan H_β line produced more precise values than the violet H_γ line. Additionally, during laboratory experimentation, the cyan H_β lines were significantly easier to locate and measure than their violet counterparts. Due to their shorter wavelength, the H_γ lines were relatively faint and often required numerous attempts to maximally center the crosshair.

As previously mentioned, the H_α line yielded two distinct clusters of values. A closer analysis of *Fig 3* reveals that the entirety of the outlier group was derived using values measured at Vernier Scale II. As such, it was critical to analyze discrepancies between the two vernier scales. *Fig 9* contains the mean θ values and mean Rydberg Constant values for each spectral line and vernier scale. The percent differences are relatively small for H_α and H_β, and slightly larger for H_γ. Furthermore, for each spectral line, the mean reading of Vernier I was larger than the mean of Vernier II. In order to evaluate the significance of these differences, hypothesis testing was performed on each set of values. Each resultant p-value was less than 0.05, indicating that the observed differences were in fact statistically significant. Additionally, the percent difference for the H_α line's theta values was the smallest, whereas the percent difference for its final Rydberg Constant values was the largest. As such, the heightened variance observed for the H_α line is likely attributed to the calibration and precision of our device. Even after scaling each vernier reading image on a computer and overlaying a ruler - each measurement only contained 5 significant figures. As such, rounding occurred at each intermediate step; incrementally impeding the precision of the final value.

VI. Conclusion

With the exception of the statistically significant differences in the readings between the two vernier scales, our observations and results aligned with what was to be expected. The mean Rydberg Constant value of 10,951,400 (1/m) ∓ 88,543.6 (1/m) was well within 10% of the

accepted value. Additionally, in order to evaluate the statistical significance of the final value, a t-test with 29 degrees of freedom was performed yielding a p-value of 0.17. This is above the $\alpha = 0.05$ threshold, meaning that there was not enough statistical evidence to reject the null hypothesis that the measured mean is equal to the actual Rydberg Constant Value. This implies that while its execution may be tedious, a mechanical telescopic spectrometer can in fact be used to accurately record the Balmer Series.

Additionally, the errors and challenges that manifested throughout the experimental process followed what was to be expected. Adhering to the principle of diffraction, the larger wavelengths of the Red and Cyan lines made it significantly easier to record their angular positions. The shorter wavelength of Violet caused higher dispersion which decreased its intensity. As such it was hard to locate and center the spectra - even in a dark room. Observed discrepancies in the recorded data were relatively consistent across each data collection round, alluding to systematic errors. This is logical as each recorded value is dependent on both the apparatus itself as well as the observer's eye. The precision of the telescopic spectrometer can be maximized through calibration, but little can be done to decrease the qualitative nature of determining when each spectral line is maximally centered.

As such, a more careful execution of this experiment would seek to increase the precision associated with centering each spectral line. Here is one plausible method, assuming that the spectrometer was already maximally calibrated. First, the size and form of the telescope's eyepiece would be measured by a caliper. A small camera with a large sensor, high ISO range, and a lens smaller than the diameter of the eyepiece could then be sourced from online retailers. Next, after measuring the dimensions of the camera's chassis, a mount could be constructed using auto-cad software and 3D printed. The camera would be mounted to the telescope arm so that its lens viewed the crosshair with no parallax. The camera's optical parameters would be adjusted to ensure maximal resolution and focus while viewing the spectral lines. Next, using basic computer vision, one could write a program that received the camera's feed as input and computed the number of pixels from the crosshair to the "boundaries" of the spectral line. The user could then manually move the telescope arm until the difference between the left and right pixel count was below some predefined threshold. This approach would remove the human error and subjectivity associated with centering the crosshair.

If one wanted to take additional measures, they could construct a high precision mechanical apparatus to pan the telescope arm. This could be accomplished by connecting a high precision pusher to the device running the computer vision program. Additional code could be written that took the left and right pixel counts as inputs, and then iteratively adjusted the pusher arm's position until the pixel difference was less than a threshold value. By having a high precision pusher arm move the telescope, the level of control over each movement would increase compared to having a human manually move it. As such, the attainable pixel difference would decrease, increasing the degree of centrality. After implementing either of these modifications, one could follow the same general process as outlined in *IV. Experiment* but without the human error associated with centering the crosshair.